Nigerian Journal of Physics (NJP)

ISSN: 1595-0611

Volume 32(2), June 2023

Implications of Fold Monitoring in Seismic Data Acquisition: Case Study of Niger Delta

***[1]Onwubuariri, C. N., [2]Anakwuba, E. K., [1]Nwokoma, E. U., [1]Dinneya, O. C., [3]Osaki L. J.**

[1]Department of Physics, Michael Okpara University of Agriculture, Umudike, Abia State, Nigeria
[2]Department of Geological Sciences, Nnamdi Azikiwe University, Awka, Anambra State, Nigeria
[3]Department of Physical and Chemical Sciences, Elizade University, Ilara Mokin, Ondo state, Nigeria

[*]Corresponding author's email: onwubuariri.chukwuebuka@mouau.edu.ng Phone: +2348033756913
ORCID: 0000-0003-3689-9065

ABSTRACT

Fold calculation and monitoring are an integral and important aspect of seismic data acquisition. Before an acquisition is carried out, so many factors must be put into consideration. These factors include grid orientation, source point (SP) and receiver point (RP) spacing, source line (SL) and receiver line (RL) spacing, source points (SP) number in each Salvo, receiver lines (RL) number in each swath, end taper, number of swaths, receiver line overlap between swaths and acquisition polygon limits. In this work, the study area was divided into 7 swaths of 12 receiver lines each, with the fold of each swath calculated in three phases which include near offset fold coverage (0 – 3650m), mid offset fold coverage (3650 – 7300m) and far offset fold coverage (7300 – 10950m). These phases of fold calculations were later merged to ascertain the full fold coverage of each swath and in turn the full fold coverage of the entire study area. The maximum fold coverage for each of the swaths within the study area ranges from 358 – 446, with average maximum fold coverage of 393.3 which is more than twice the minimum fold coverage expectancy (180) for the study area. Fold calculations were carried out, while the lateral extent where full fold coverage is experienced within each swath was noted. It was also observed that where the full fold coverage of one swath ends, the full fold of another swath begins. This implies that when all the swaths are merged, no fold drop will be experienced, unless at the tapering ends of the entire study area.

Keywords:
Fold,
Swath,
Bin Size,
Offset,
In-line,
Cross-line

INTRODUCTION

Primarily, the basic aim of seismic surveys is to record with high precision the ground motion generated by a known source within a known location. When ground motions are recorded with time, it is said to make up a seismogram and actually, this is the core information needed for interpretation through imaging or modeling (Cordsen et al. 2000). For every acquisition project, stipulated fold coverage is expected in order to get the desired result. In this research work, a close monitor of the fold coverage was carried out, area of full fold and fold drops were noted, their implications and how it affects the entire project. A 3D grid design was used in this acquisition project.

Prior to successful seismic data acquisition program, a detailed and careful planning is needed to be carried out and such planning is as stipulated below (Gadallah & Fisher 2009):

i. Selection of main and other targets.
ii. Prospect of production estimation and gain.
iii. Acquisition costs.
iv. Specification of goals and project priorities.
v. Setting data quality requirement.
vi. Schedules and deadlines.
vii. Maps with superimposed lines of survey.
viii. Acquisition method and equipment selection.

3D Acquisition

In the recent times, seismic surveys are carried out in 3D format. 2D acquisitions are barely carried out now due to its flaws which include misrepresentation of the image of geologic structures and poor subsurface sampling to elucidate little geologic features. Figure 1 expresses the problem of distortion which assumes that all reflections emanates vertically below the seismic lines as observed in 2D shooting.

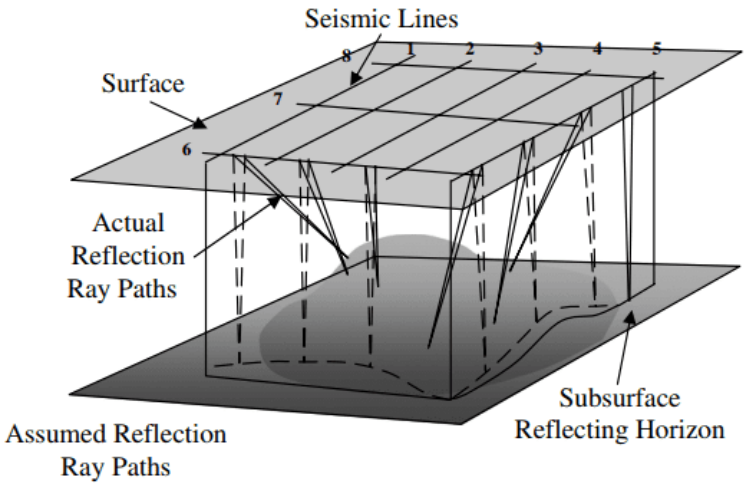

Figure 1: Real and presumed ray paths from a subsurface horizon of 2-D case (Gadallah & Fisher 2009)

In this case, the reflecting surface has a dome shape. Lines 5 and 6 from Figure 1 show a 2D reflection ray path. The places reflections actually took place in Figure 1 are noted with solid lines, and the broken lines in the vertical plane show the assumed ray paths passing across the lines. The actual cross section of the structure is the solid curve below line 5 and the apparent cross section is represented by the dashed curves. It is observed that the true structure passing through line 6 in the vertical plane is flat. The erroneous cross section indicated by the curved broken line below line 6 assumes that the reflection ray paths were all in vertical plane. Generally, 2D data interpretation expresses a reflecting surface which is completely different when compared to the exact position. It also possesses less dip than the exact reflecting surface. 2D can be accommodated for reflecting surfaces that are flat or have very small dip. However, sufficient trapping capacity for commercial quantity of petroleum is not seen such structures.

Fold

Trace counts which make up a single stack trace, that is, the number of midpoints within a Common Mid Point (CMP) bin, are known to be stacking fold and they account for the number of midpoints overlapping area (Claerbout, 1976). Fold is the number of times a bin is sampled. It plays a huge role in the control of signal-to-noise ratio (S/N). To accomplish about 40% increase in signal-to-noise ratio, fold must be enlarged twice as shown in Figure 2. To make signal-to-noise ratio have twice its value, the fold will be multiplied by 4 as the noise is randomly disseminated in a Gaussian manner (Cordsen & Lawton 1996).

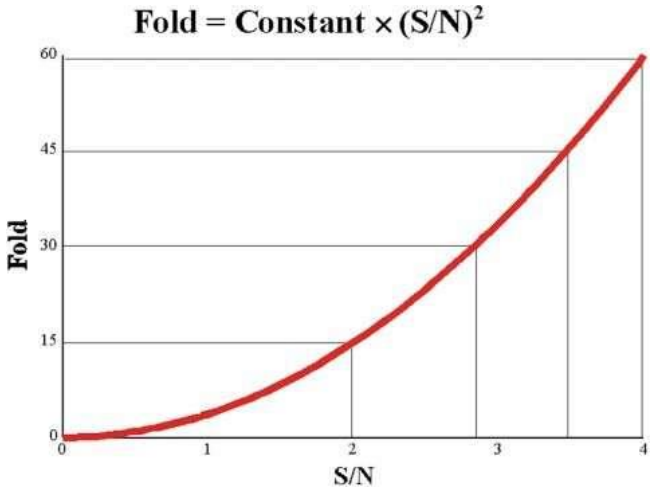

Figure 2: Fold versus signal-to-noise ratio (S/N) (Cordsen et al. 2000)

According to Krey (1987), the proportion of 3D to 2D fold relies on frequency and as well has variation as expressed in equation (1)

$$3-\text{D fold} = 2-D\ fold \times frequency \times C \quad (1)$$

Where C is an arbitrary constant.

Note that 3D fold is always relatively higher in achieving results when compared to 2D imaging and this occurs when the spacing of 2D is far lesser as compared to the bin size of 3D (Mike Galbraith, 2001). To support a lower 3D fold, it is of necessity to consider sampling density rather than the density of geophone station. When we have larger geophone numbers present in a group, the subsurface is sampled more densely and this will in turn improve data quality (Cordsen & Lawton 1996). When considering sources, sweep effort per square kilometer is also considered. Sweep effort is defined as shown in equation 2

$$S/N\ improvement\ in\ dB = 20\log[number\ of\ vibrators \times fundamental\ ground\ force \times (sweep\ length \times number\ of\ sweeps \times bandwidth\ of\ sweep)^{1/2}] \quad (2)$$

Fold can be calculated in various ways. It is a fact that a source point can generate several midpoints for different recording channels. When all the offsets are situated within acceptable recording range, the basic fold equation is as expressed in equation 3

$$Fold = SD \times NC \times B^2 \times U \quad (3)$$

Where SD is the number of source points per unit area, NC is the number of channels, B is the bin dimension (for square bins), and U = units factor (10^{-6} for m/km^2; 0.03587 x 10^{-6} for ft/mi ^{2}).

Equation 3 is an easy approach to calculating average fold. To determine fold adequacy, there will be need to evaluate the different fold components. Considering orthogonal geometry, the stacking fold is completely defined by the highest offsets of both in-line and cross-line alongside the receiver and source line gaps. Disparity in the choice of station spacing will have no effect on fold, but will affect the bin size, source density and number of channels needed.

In-line Fold

When considering a straight-line survey that is orthogonal, in-line fold can be expressed as follows:

$$\text{In-line fold} = \frac{number\ of\ receivers\ x\ station\ interval}{2\ x\ source\ interval\ along\ the\ receiver\ line} \quad (4)$$

Or

$$\text{In-line fold} = \frac{number\ of\ receivers\ x\ RI}{2\ \text{x SLI}} = \frac{in-line\ patch\ dimension}{2\ X\ SLI} \quad (5)$$

In this case, the source line interval (SLI) determines how many source points that will be situated along any receiver line. Therefore, it becomes imperative to use (number of receivers) $\mathbf{x}$ (RI) in equation 5 in defining the midpoint area that is covered. All receivers are expected to be within the maximum usable offset range in equations 5 and 6.

Cross-line Fold

Similarly, cross-line fold is given as:

$$\text{Cross-line fold} = \frac{\textbf{Source line length}}{\textbf{2 x Reciever line Interval}} = \frac{\textbf{cross-line patch dimension}}{\textbf{2 x RLI}} \quad (6)$$

$$= \frac{\textbf{number of receiver lines x RLI}}{\textbf{2 x RLI}} = \frac{\textbf{NRL}}{\textbf{2}} \quad (7)$$

With respect to cross-line, it is of essence to employ (number of receiver lines) x (RLI) in equations 6 and 7 in expressing the covered mid-point area. Cross-line fold can simply be expressed as the number of active receiver lines divided by two (2) within the recording patch. Figure 3 indicates cross-line fold possessing an active source line (shown in red) across the receiver lines.

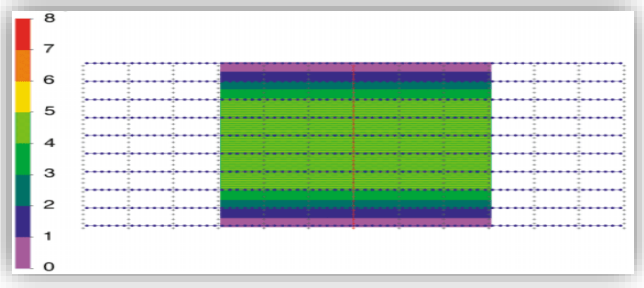

Figure 3: Cross-line fold of 10 x 72 patch (Cordsen et al. 2000)

Total Fold

Multiplying in-line fold and cross-line fold simply gives the total 3D nominal fold. This is expressed in equation 8

Total Nominal Fold = *(in-line fold) x (cross-line fold)* (8)

In equation 8, it is assumed that the bin size is constant, therefore equating half of the receiver interval, which also equals half the source interval. With all the source points being within the patch, they are laid orthogonally. If the numbers of active receiver lines are even, the cross-line fold becomes an integer which gives rise to a smooth cross-line distribution of fold. When the maximum stack offset goes beyond any source point offset to any receiver station within the patch, it will give rise to the smoothest fold distributions, provided that the in-line and cross-line folds are integers (Cordsen & Lawton 1996). The design principles observed at this point is described in equations 9 and 10 respectively.

$$\text{In-line fold} = \frac{In-line\ patch\ dimension}{2\ x\ SLI} \quad (9)$$

$$\text{Cross-line fold} = \frac{Cross-line\ patch\ dimension}{2\ x\ RLI} \quad (10)$$

Therefore, total fold is given by the multiplication of equations 9 and 10. Note that the patch size is given by the product of In-line patch dimension and Cross-line patch dimension. Also, box size is given by the product of Receiver Line Interval and Source Line Interval.

$$\textbf{Total Fold} = \frac{(In-line\ patch\ dimension)x(Cross-line\ patch\ Dimension)}{(2\ x\ SLI)(2\ X\ RLI)} \quad (11)$$

$$\textbf{Total fold} = \frac{Patch\ Size}{4\ x\ Box\ Size} \quad (12)$$

The above expression is real for rolling stations and lines on/off. It is also worthy of note that one-quarter (1/4) of the patch size equals the area in the subsurface that is covered by midpoints. Therefore, to roll the receiver stations and lines, the quarter patches of midpoints overlap to build up the fold.

Since the ratio of the area of a circle and a square patch is given as πR^2 (patch size), the fold within a circle of radius R is expressed as equation 13. Equation 13 can be compared to equation 12

$$Fold_R = \pi R^2 / (4 \text{ x SLI x RLI})$$

$$= \pi R^2 / (4 \text{ x Box Size}) \quad (13)$$

This expression predicts each horizon (depth) of interest fold as defined by that horizon's mute function (or X_{mute}). Equation 13 can be used to calculate fold of circular patches as well. Note that equation 13 is totally independent of the station spacing.

At a given offset R, Goodway and Ragan (1995) compared 2D fold and 3D fold. For 2D data, the fold is calculated as

$$\text{2-D fold}_R = \frac{Offset\ R}{Source\ Interval} \quad (14)$$

The ratio of 3D and 2D fold at offset R can then be defined as

$$\text{Fold Ratio}_R = \frac{\pi R(2-D\ Source\ Interval)}{4\ x\ SLI\ x\ RLI} \quad (15)$$

This fold ratio is linear with offset R. Low fold ratio results from large line (coarse sampling) and this might be accepted for deeper targets. To increase the fold ratio, line spacing must decrease, thereby increasing near offset fold, which is healthy for shallow targets.

Fold Taper

Fold taper is a vital factor to be considered when calculating fold. The area where full fold is experienced is described by this parameter. The width of this strip which needs to be calculated differently is not often the same in the in-line and cross-line directions (O'Connell et al, 1993).The fold taper, by approximation, equals one quarter of the patch dimension in the fold-taper direction.

Signal-To-Noise Ratio (S/N)

When considering square bins, the length of one side of the bin is seen to be directly proportional to signal-to-noise ratio (S/N) as shown in Figure 4. Therefore, slight change in bin size selection can have tremendous impact on the fold and the S/N. When fold drops below the required or estimated level for a few bins, it does not necessarily imply that the 3D survey was poorly designed, as there are some factors that can cause fold drop. Also note that to increase the fold of a well-designed survey by small percentage will attract extra cost just to compensate for the fold drop of a few bins.

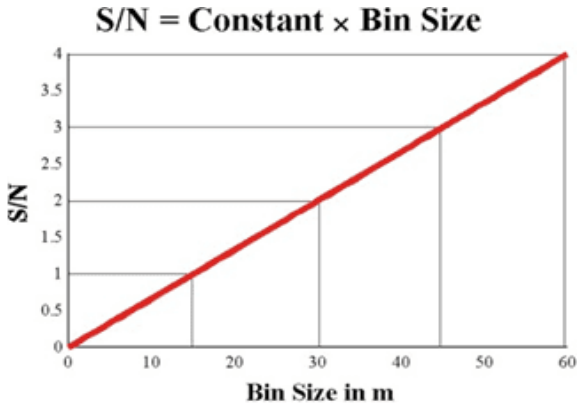

Figure 4: Signal-to-noise ratio (S/N) versus bin size (Cordsen et al. 2000)

Bin Size

Bin size is not the same as bin interval; therefore, it is important to differentiate the two. Traces are stacked within the bin size while bin interval determines the distance of display of trace summations. It has been observed that mostly, bin size (dimension) and bin interval are used interchangeably. This is as a result of both having the same value, but this may differ occasionally (e.g. flex-binning in marine surveys).

Bin size and fold cannot be separated; therefore, they go hand in hand. Figure 5 shows that fold is a quadratic function of length on one side of the bin.

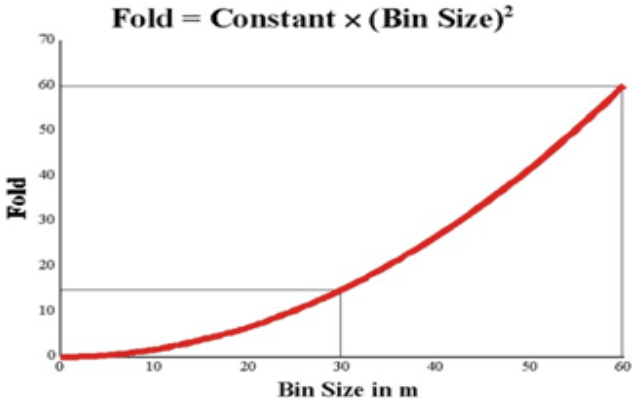

Figure 5: Fold versus bin size (Cordsen et al. 2000)

Equation 16 is the basic fold equation which is derived to indicate that the constant relating fold to (bin size)^2 is the midpoint density (i.e., the number of midpoints per square unit area). This equation is as expressed below:

$$\text{Fold} = \text{SD} \times \text{NC} \times \text{B}^2 \qquad (16)$$

Where SD is the number of source points per unit area, NC is the number of channels, B is the bin dimension (for square bins).

Square shape is the preferred shape of a 3D data bin. Rectangular bins may be considered for the purpose of exposing certain geologic features where different lateral resolutions are required for different directions. Requirement for spatial sampling for migration may also differ in different directions. Cost issues most often determines a different receiver station than interval of source point and this will cause a difference in the nature of bin size. Having little number of subsurface measurements in the long direction or arm of the bin which limits the resolving power of geological features in that direction, is the deficiency rectangular bins may cause.

MATERIALS AND METHODS

Study area

The study area is located in some parts Bayelsa and Rivers State. It comprises of seven local government areas, namely; Ahoada West LGA, Abua/Odua LGA in Rivers State and Kolokuma/Opokuma LGA, Sagbama LGA, Yenagoa LGA, Ogbia LGA in Bayelsa State.

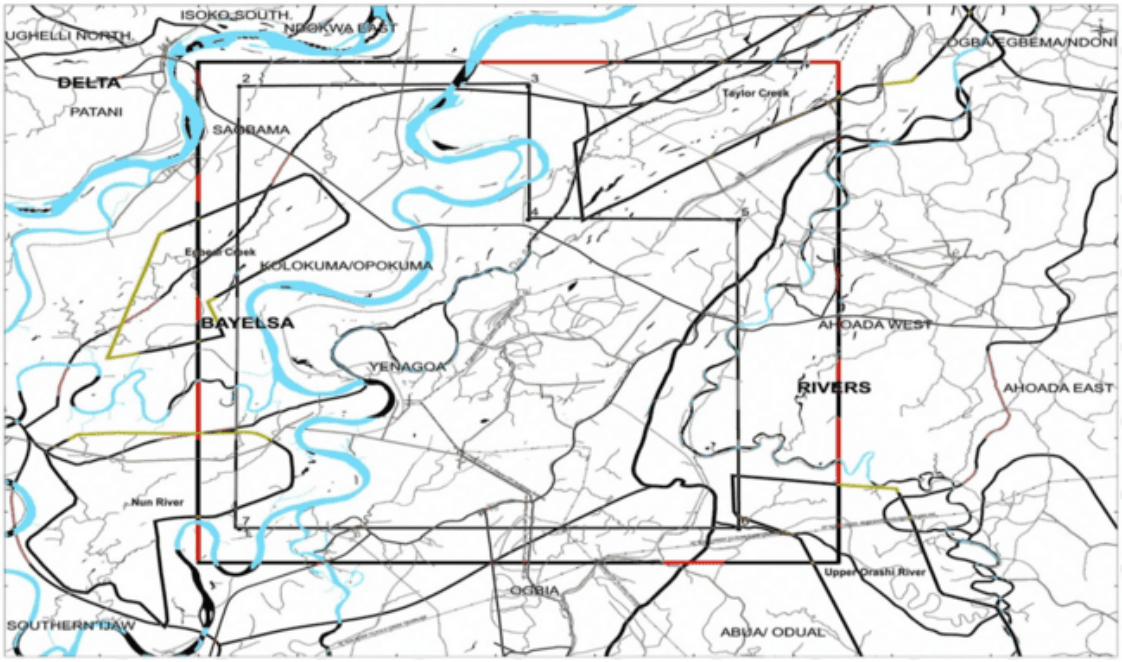

Figure 6: Map of the study area

Generally, the vegetation is about 60% upland rain forest in the southeastern and northeastern part and about 40% mixture of swampy raffia palm and floating grass towards the sloppy channels of the Orashi River and Nun River in the southwest. Pockets of marshy swamps were found close to streams and water channels. Most part of the prospect is surrounded by highland and some low areas are dominated with light shrubs, thick rain forest, and swamp with palm and raffia trees in some places. Several ponds and lakes were noticed which remain active all through the year. Due to thick vegetation in North western part of the study area, logging is observed in most part. River Nun intersects the study area at southwestern end, and Orashi River at the southeastern part of the study area.

The terrain is mainly sandy and muddy with predominantly dry high land and low-lying swampy forest while the topography in the study areas is undulating. There is no clear-cut area of high and low land and as a result, both rain and flood that are trapped at the depressed portions thereby creating marshy and swampy terrains in some parts of the study area.

Acquisition design

The study area was designed in a 3D format to provide an improved symmetrical seismic data output for a more structural imaging of the field, understand its fluid distribution and evaluate the exploration potential of the study area. The design also provides proper azimuth, offset distribution and better multiplicity for enhanced velocity analysis, multiple attenuation, static solutions (for azimuth dependent variations arising from dip or anisotropy) and more directional sampling of the subsurface (Geoscience Training Center 2002).

The primary objectives of this seismic acquisition are:

i. Detecting hydrocarbon movements through 4D reservoir monitoring,
ii. understanding fluid distribution,
iii. improving the structural imaging of the field,
iv. achieving optimum resolution (signal to noise ratio) at the deeper levels
v. improving the understanding of fluid distribution in the field via AVO/QI techniques
vi. fully evaluating deep exploratory potential of the study area.

The parameters defined in this design include the grid orientation, source point (SP) and receiver point (RP) spacing, source line (SL) and receiver line (RL) spacing, number of source points (SP) per Salvo, number of receiver lines (RL) per swath, end taper, number of swaths, receiver line overlap between swaths and acquisition polygon limits.

For this study, a receiver spread of 4368 channels broken into twelve lines of 364 groups each was used, except for the tapering off ends. 45 shots at the left side of the active spread, 77 shots within the spread and 46 shots at the right side of the spread made up the shooting salvo of one hundred and sixty eight (168) shots, centered on the spread. This results to a cross spread geometry of 12 lines X 364 channels X 168 shots. The source/receiver geometry generates full fold coverage of 312 and with a maximum offset of 10990.05m.

The survey block consists of 84 receiver lines at 0° orientation and 98 source lines at 90° orientation. Receiver line spacing is 350m while source line spacing is 350m. Receiver points are at intervals of 50m and source points are equally at 50m interval.

Based on the chosen parameters for this study, terrain type, vegetation, and information from previous acquisitions carried out, the following parameters were used to acquire the 3D data:

i. The shot points consist of a Single Deep Hole (SDH) at 42m
ii. 2Kg charge size were used as energy source per source point
iii. Airgun shots were taken in the major creeks with a capacity of 460 cubic inches at 2000 p.s.i. at each location.
iv. Marsh geophones and hydrophones were used for recording, depending on the terrain condition of the receiver points.
v. Single hydrophone anchored to the riverbed was used for receiver station in water.
vi. Two strings of geophone each with 9 jugs connected in series and spaced 2.78m interval parallel to the receiver station were used for receiver station on land. However, for stations at creek edges (or other obstacles), the geophone strings were bunched.
vii. UNITE cable-less acquisition system was deployed at heavily built-up region where cable units cannot be practicable

Study area boundary

The study area is as represented with their coordinates in Table 1, with the vertexes shown in Figure 7.

Table 1: Coordinates of the study area

S/No	Vertex	Easting	Northing
1	A	422070.00	105910.00
2	B	422070.00	131350.00
3	C	436640.00	131350.00
4	D	436640.00	124730.00
5	E	447270.00	124730.00
6	F	447270.00	105910.00

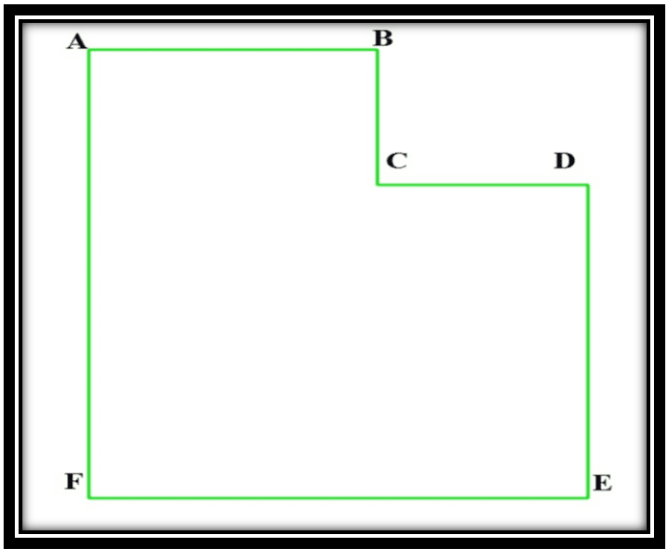

Figure 7: The vertexes of the study area with their coordinates listed in Table 1

RESULTS AND DISCUSSION

Fold coverage analysis and presentation of the study area

For acquisition convenience, the study area was divided into swaths and below is the fold analysis of swaths under consideration. These fold analyses are done for near offset, mid offset and far offset. A combined fold analysis (combination of near offset fold, mid offset fold and far offset fold) was also carried out to determine if there are areas of fold drop as specified by the project design. This will help the planning seismologist to know if there will be need to plant some infill shots to compensate for fold drop (Yilmaz 2001).

The fold coverage maps on display as seen in Figs.8-32 represent the order of coverage for each bin with different colours. This computation is done using MESA Expert Software, version 10.04.

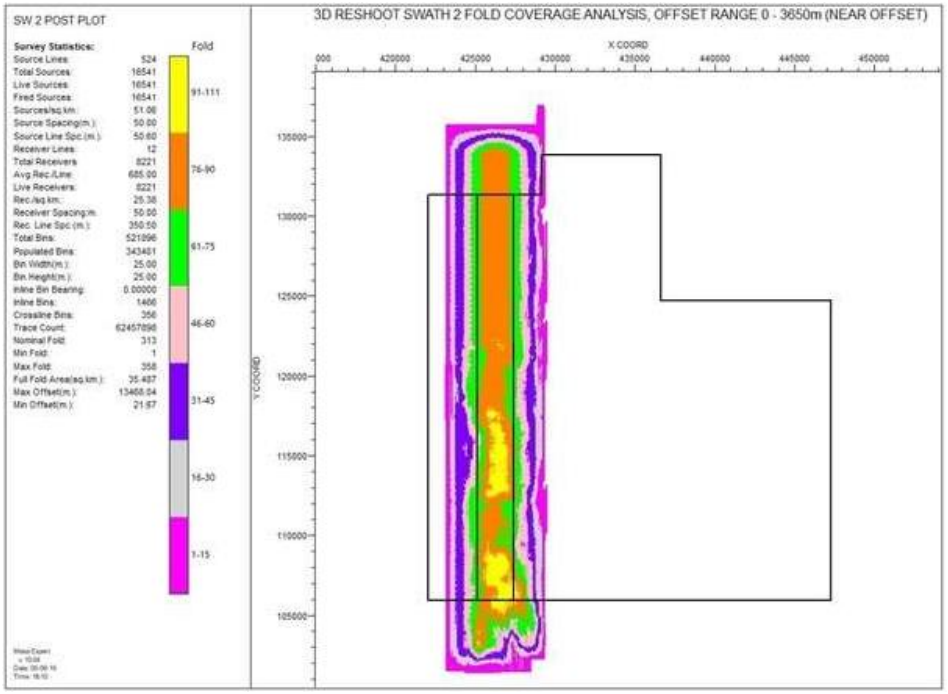

Figure 8**:** Swath 2 near offset fold coverage (0 - 3650m)

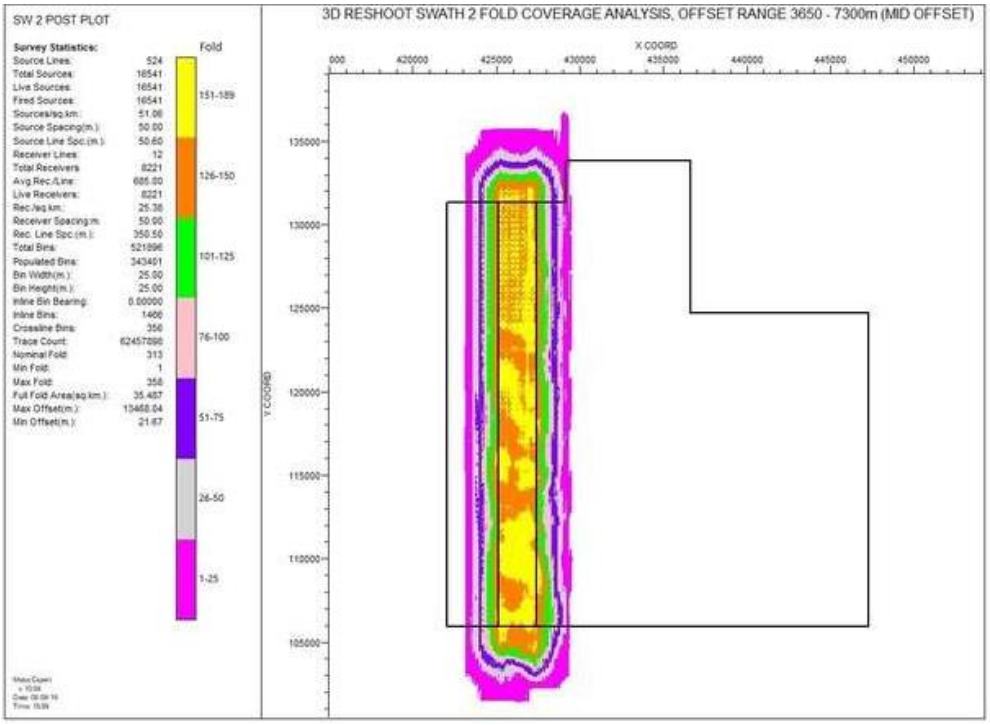

Figure 9: Swath 2 mid offset fold coverage (3650 - 7300m)

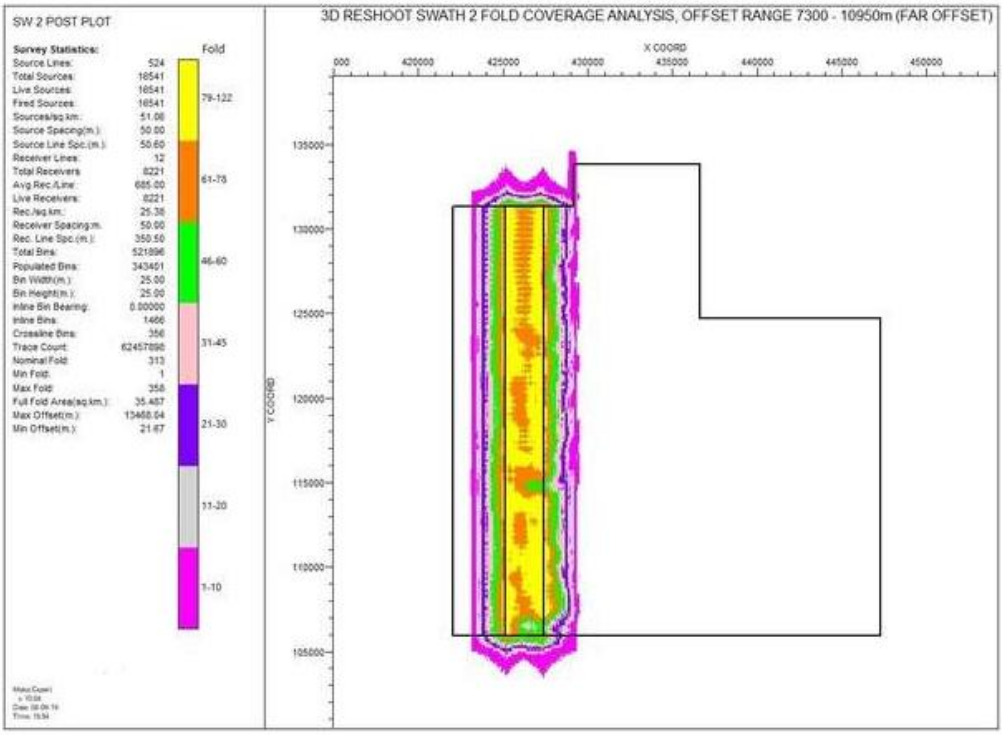

Figure 10**:** Swath 2 far offset fold coverage (7300 - 10950m)

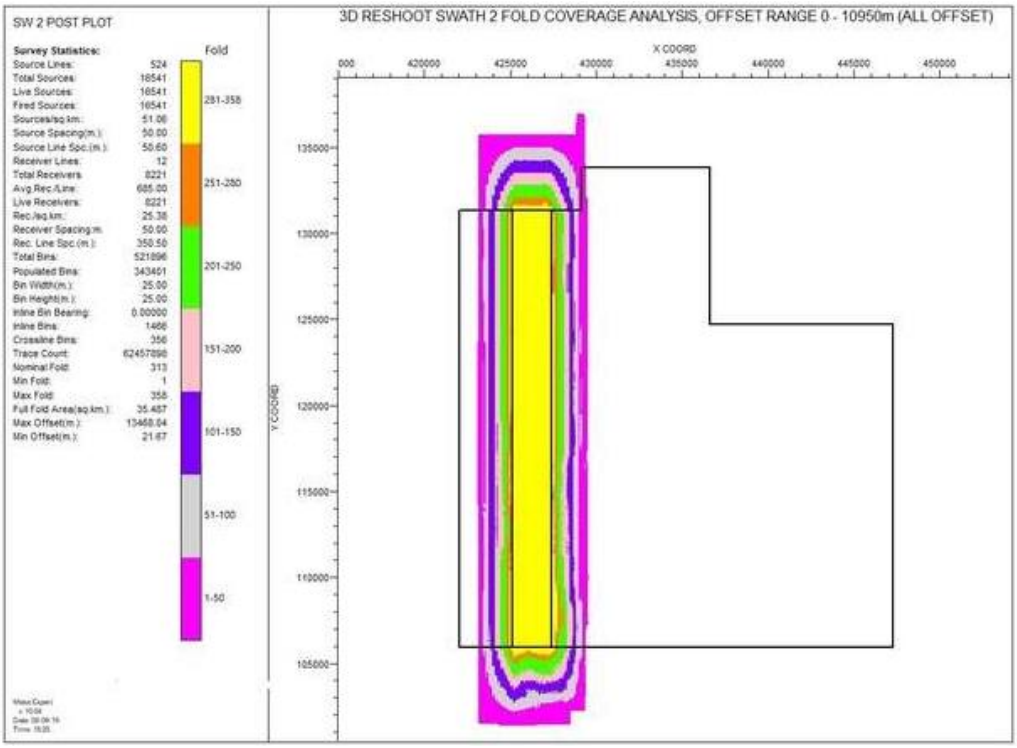

Figure 11: Swath 2 all offset fold coverage (0 - 10950m)

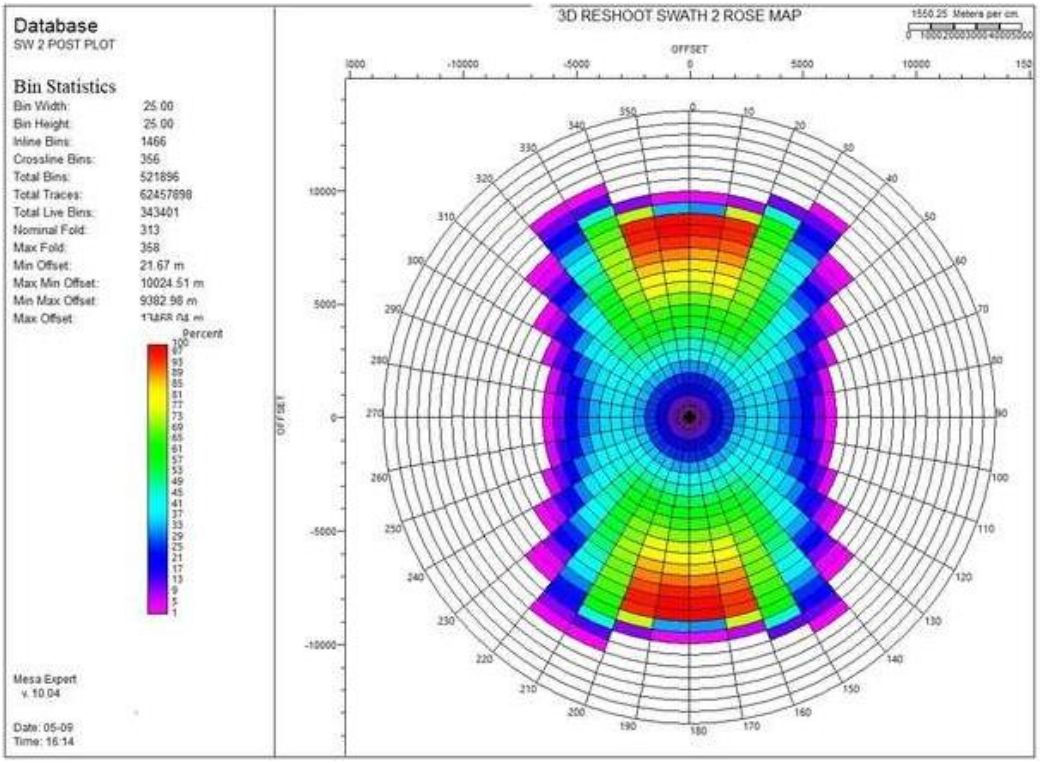

Figure 12: Swath 2 Rose diagram

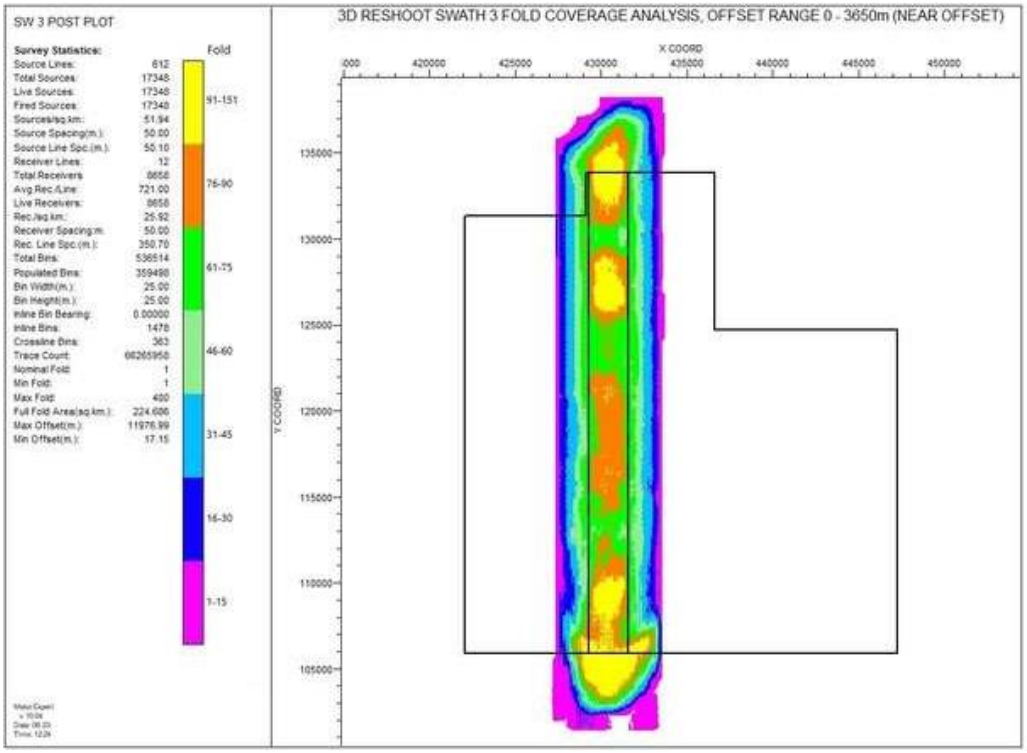

Figure 13: Swath 3 near offset fold coverage (0 – 3650m)

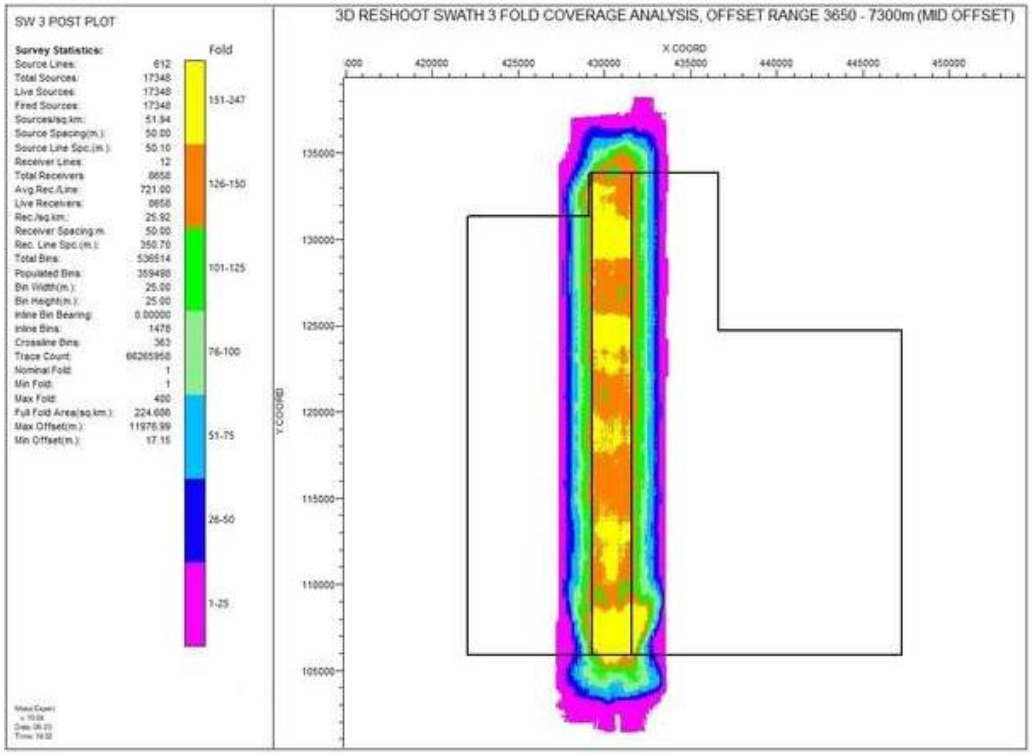

Figure 14: Swath 3 mid offset fold coverage (3650 - 7300m)

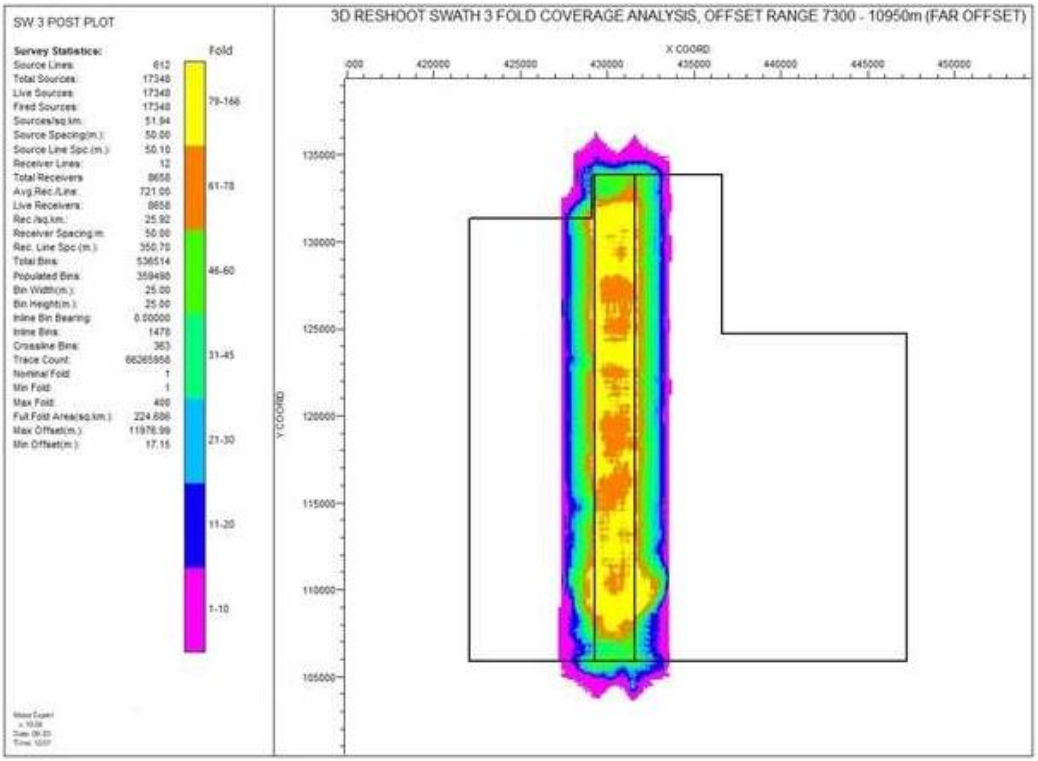

Figure 15: Swath 3 far offset fold coverage (7300 - 10950m)

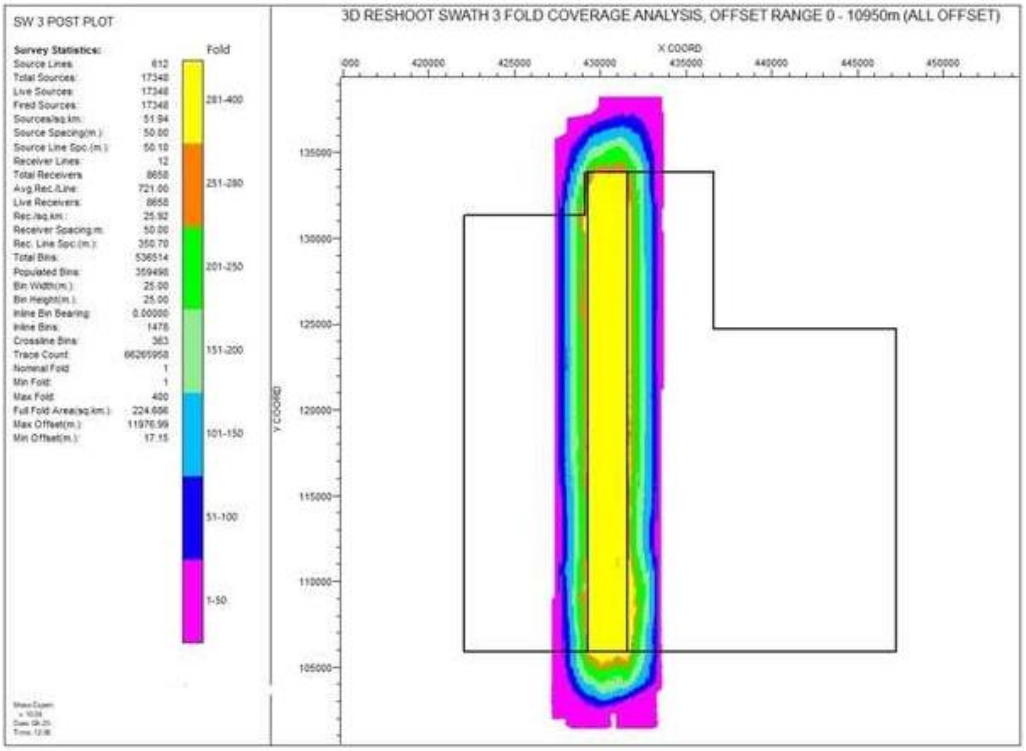

Figure 16: Swath 3 all offset fold coverage (0 - 1950m)

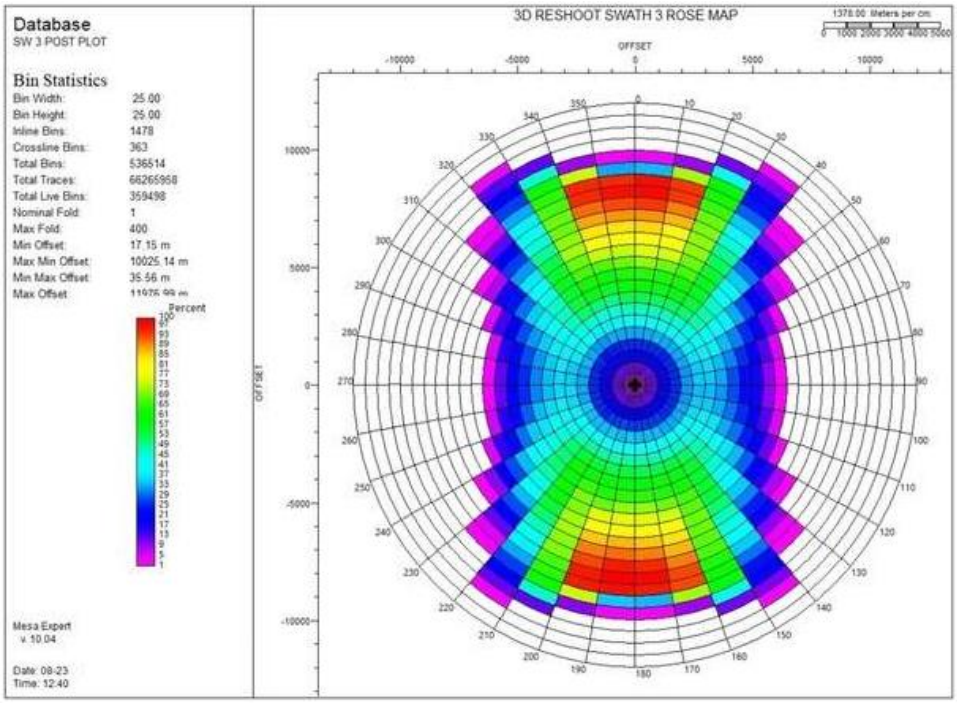

Figure 17: Swath 3 Rose diagram

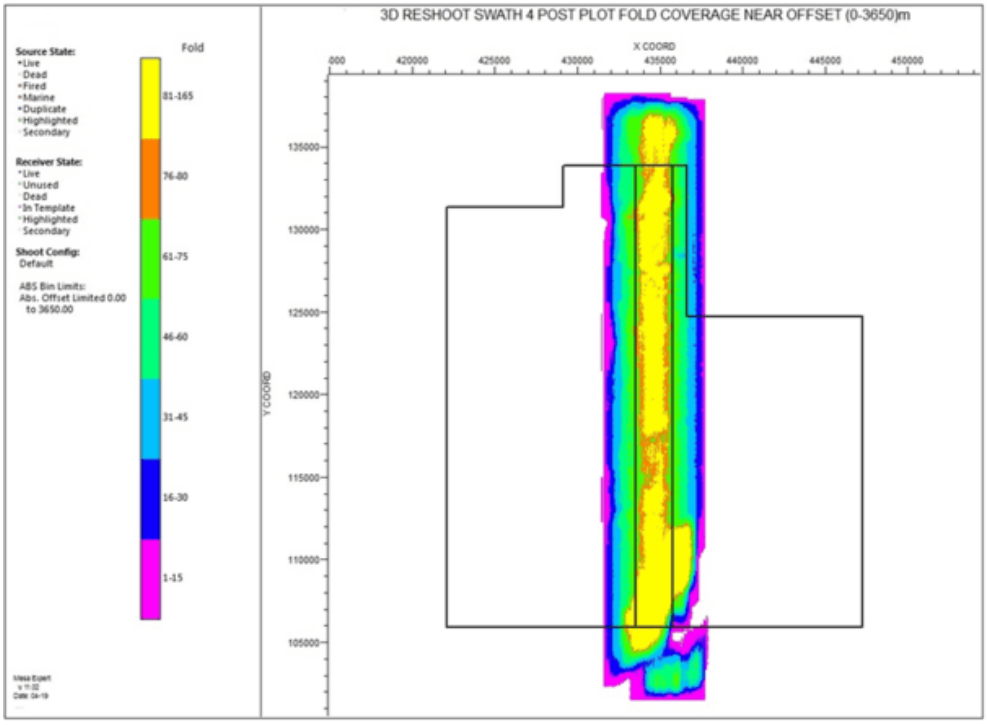

Figure 18: Swath 4 near offset fold coverage (0 – 3650m)

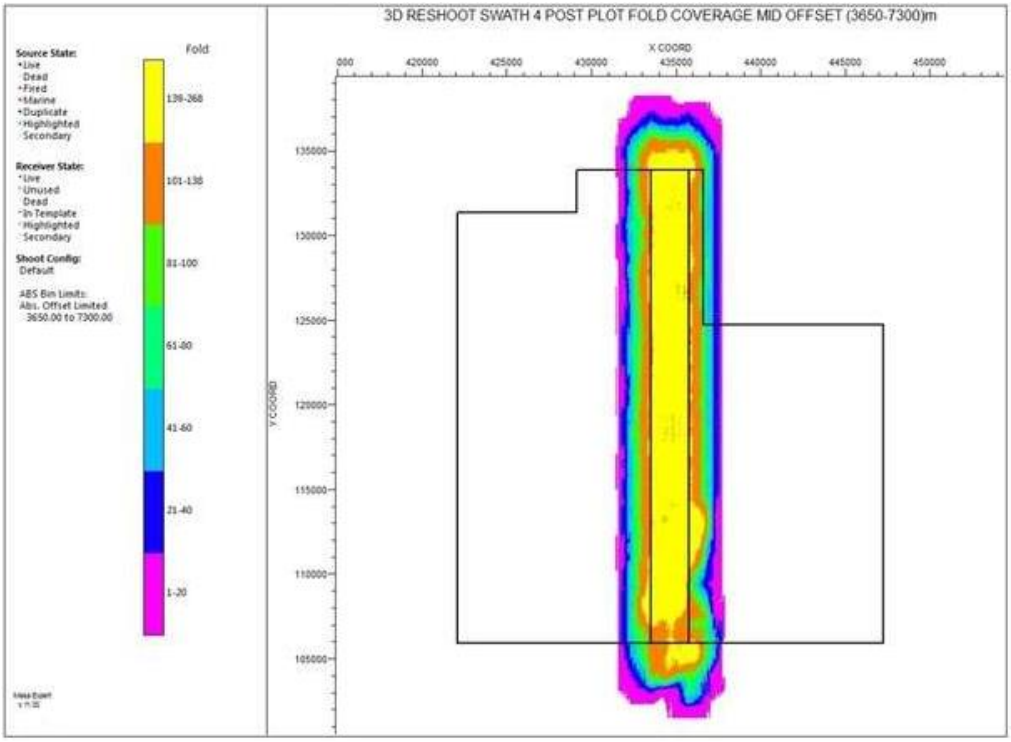

Figure 19: Swath 4 mid offset fold coverage (3650 7300m)

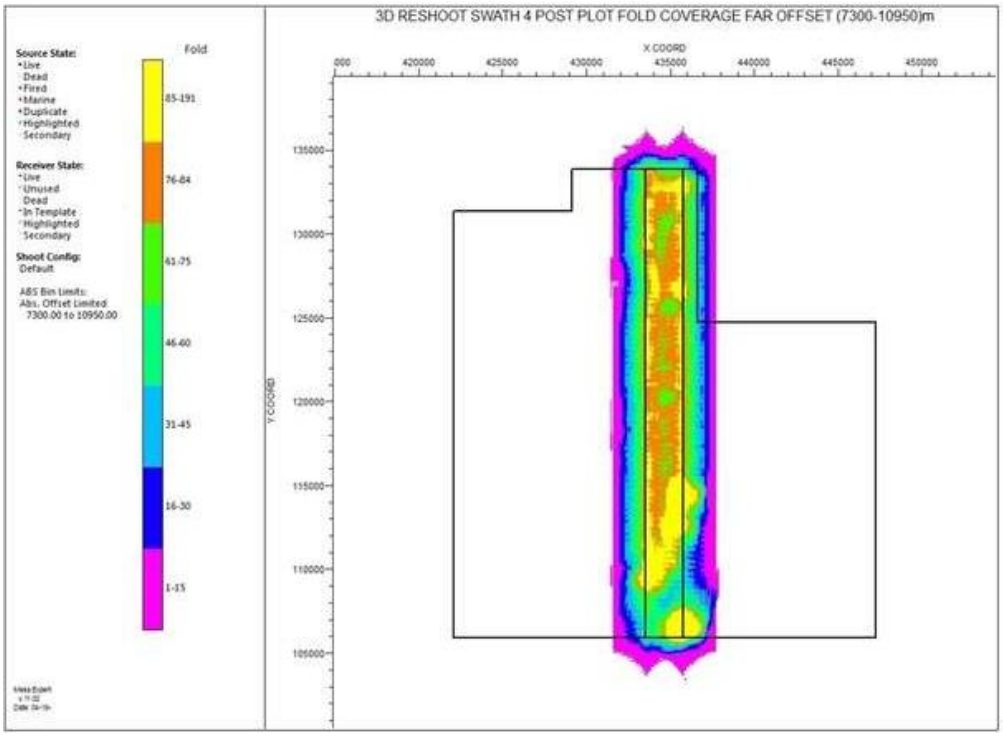

Figure 20: Swath 4 far offset fold coverage (7300 – 10950m)

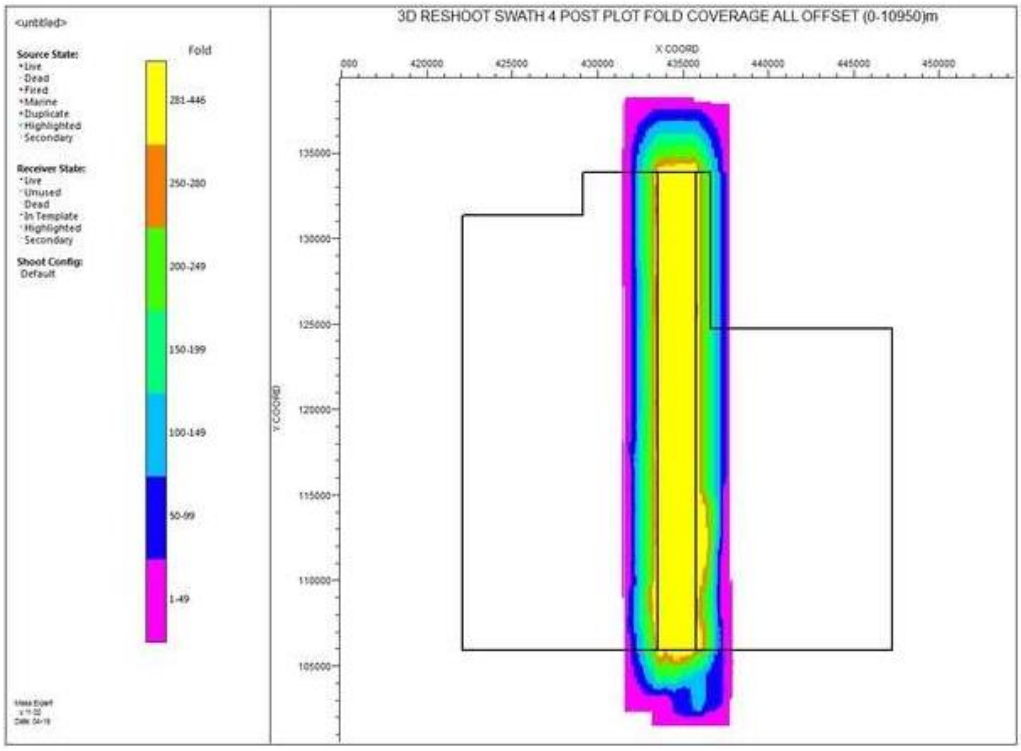

Figure 21: Swath 4 all offset fold coverage (0 – 10950m)

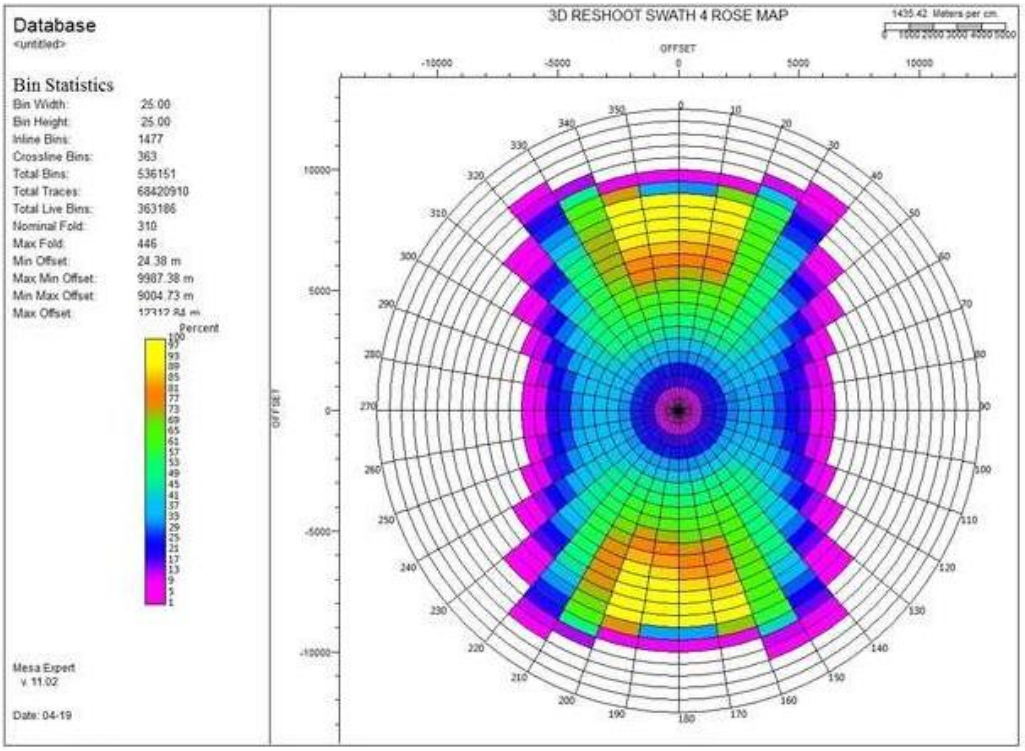

Figure 22: Swath 4 Rose diagram

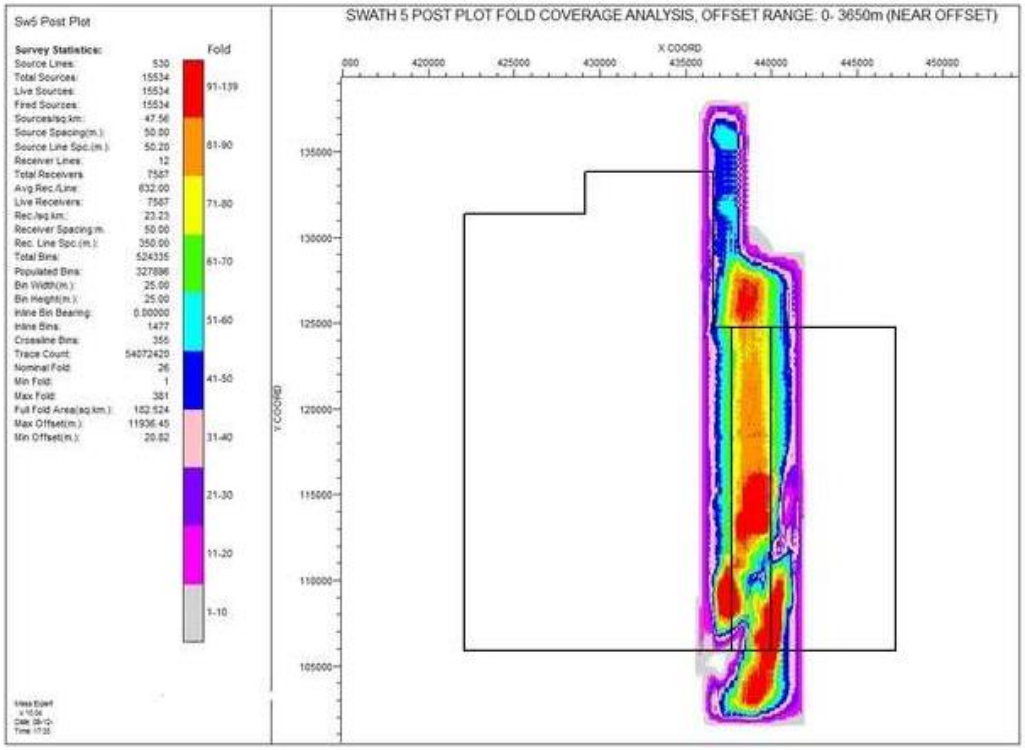

Figure 23: Swath 5 near offset fold coverage (0 – 3650m)

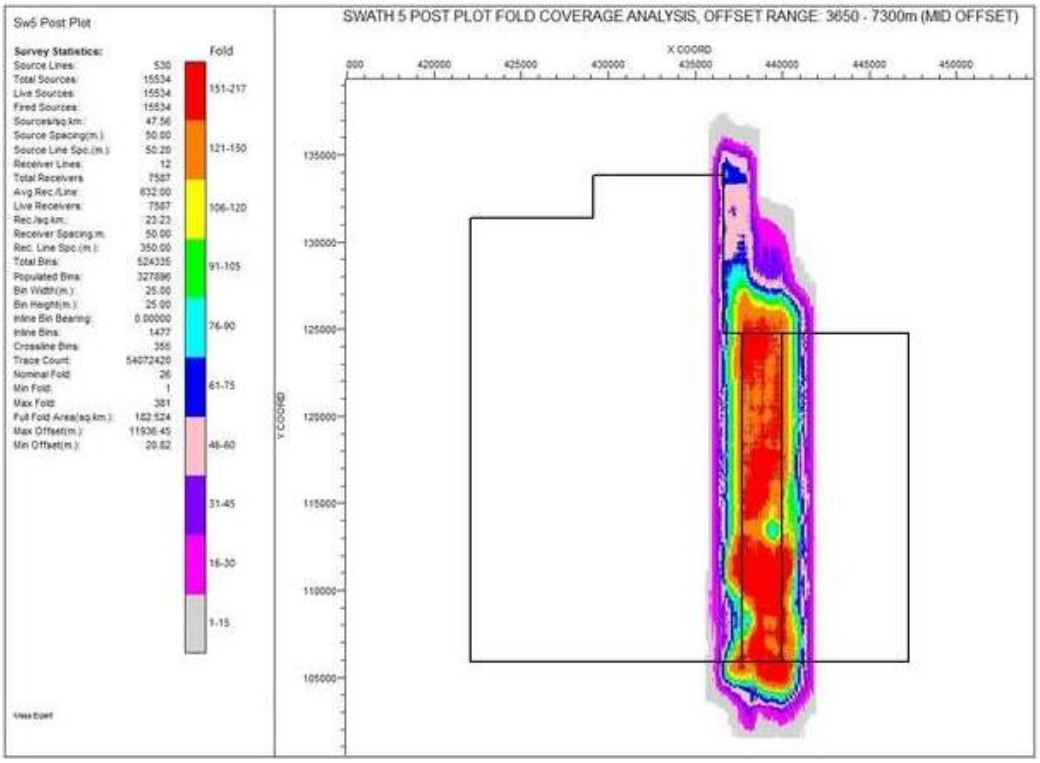

Figure 24: Swath 5 mid offset fold coverage (3650 - 7300m)

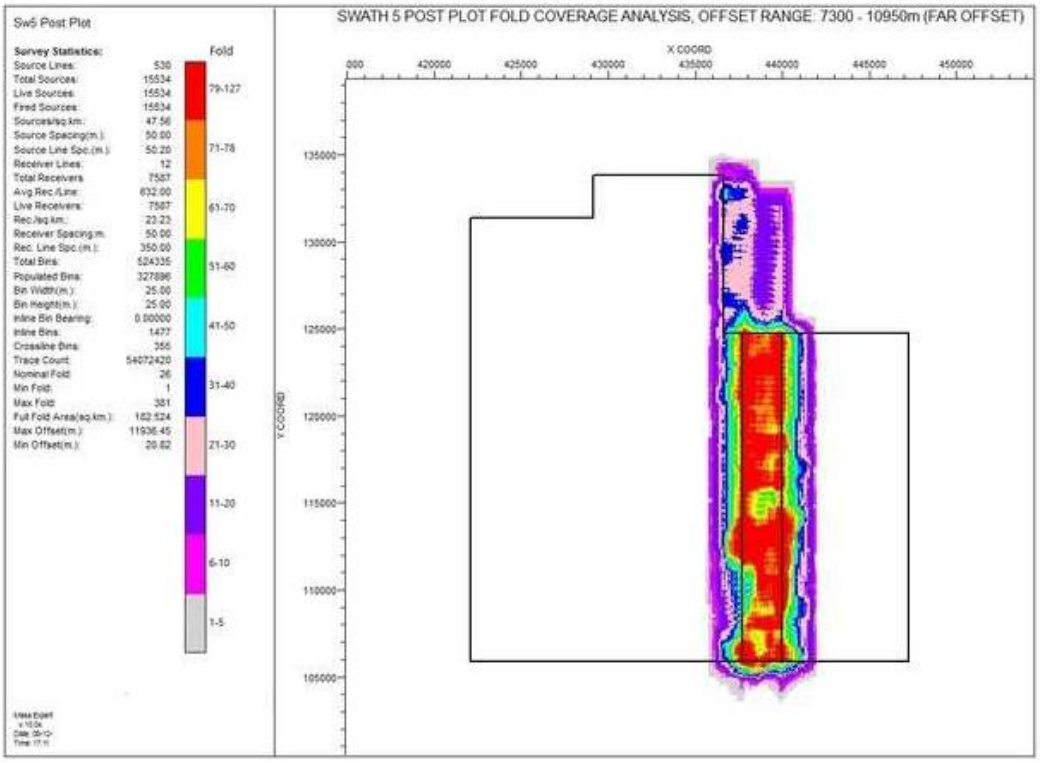

Figure 25: Swath 5 far offset fold coverage (7300 – 10950m)

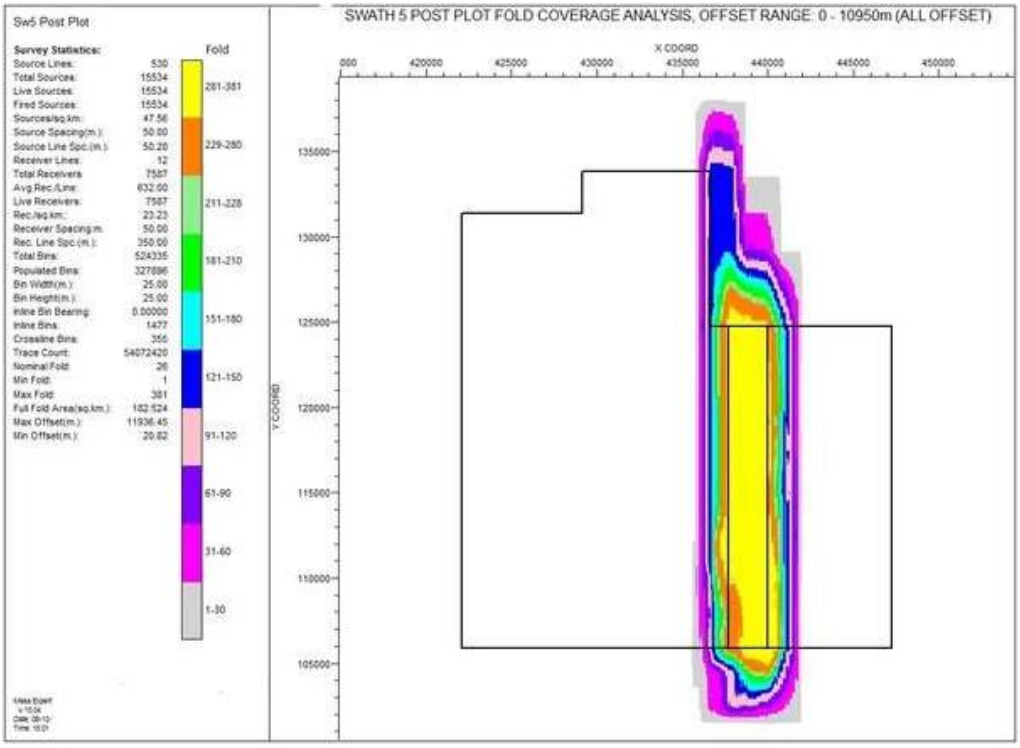

Figure 26: Swath 5 all offset fold coverage (0 – 10950m)

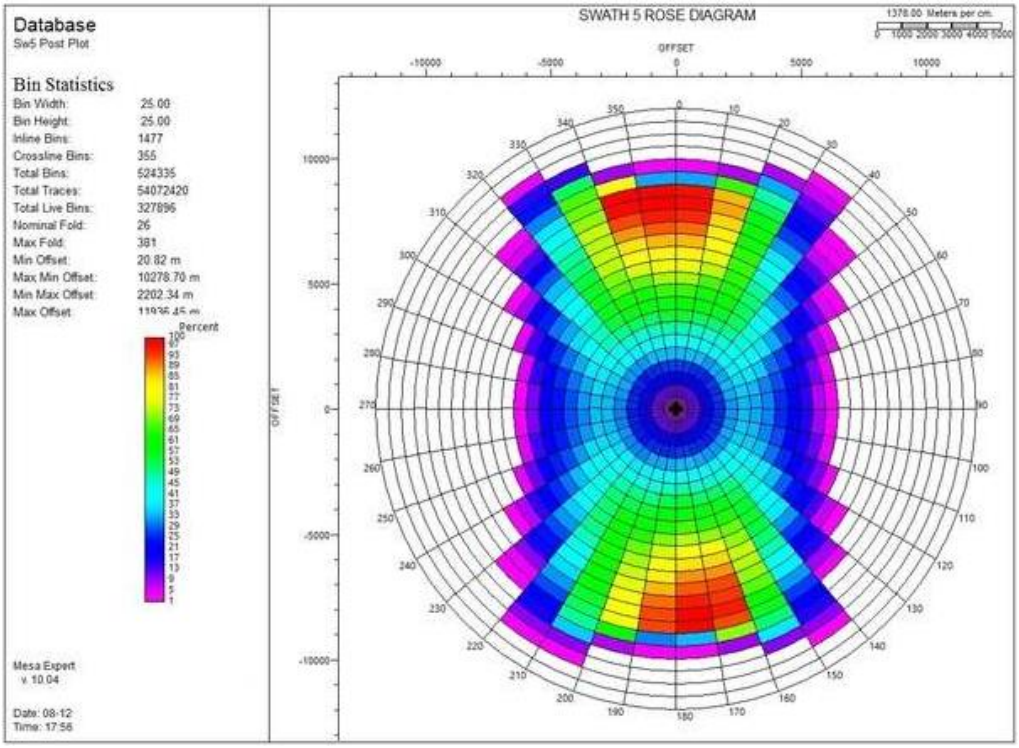

Figure 27: Swath 5 Rose diagram

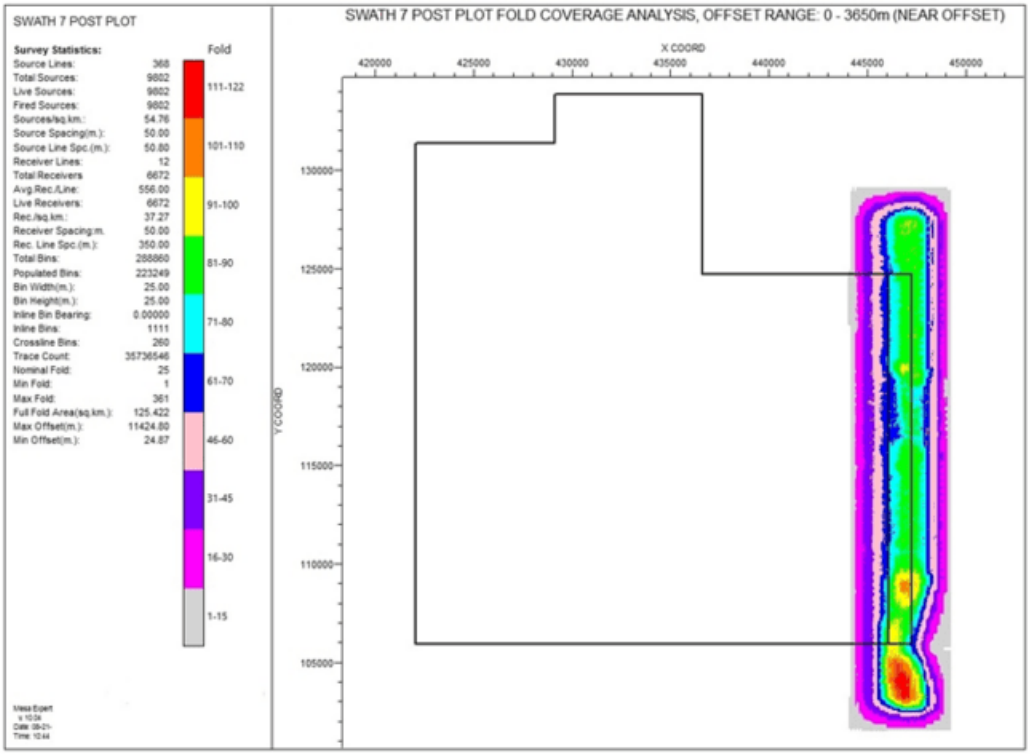

Figure 28: Swath 7 near offset fold coverage (0 – 3650m)

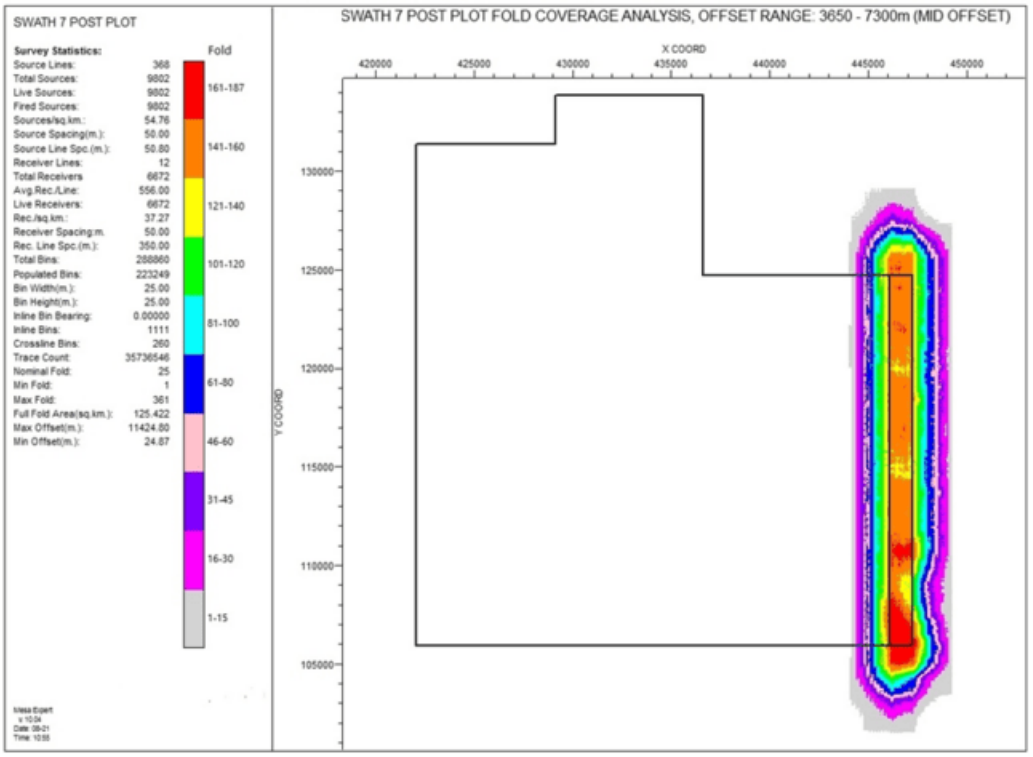

Figure 29: Swath 7 mid offset fold coverage (3650 - 7300m)

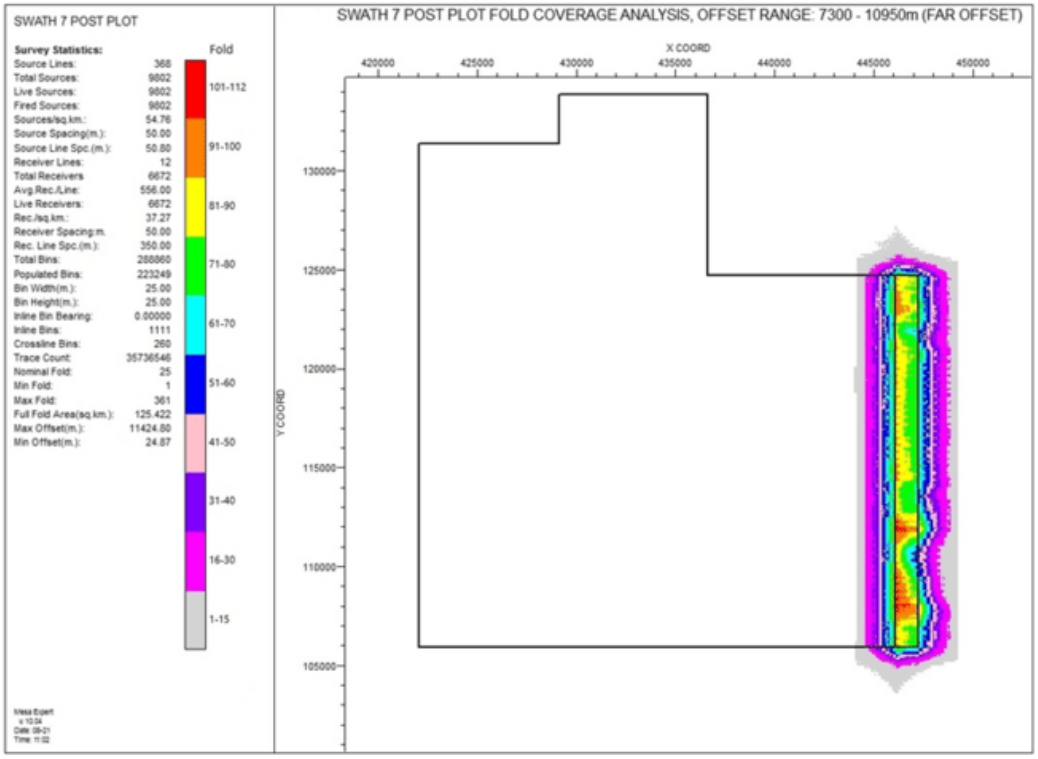

Figure 30: Swath 7 far offset fold coverage (7300 - 10950m)

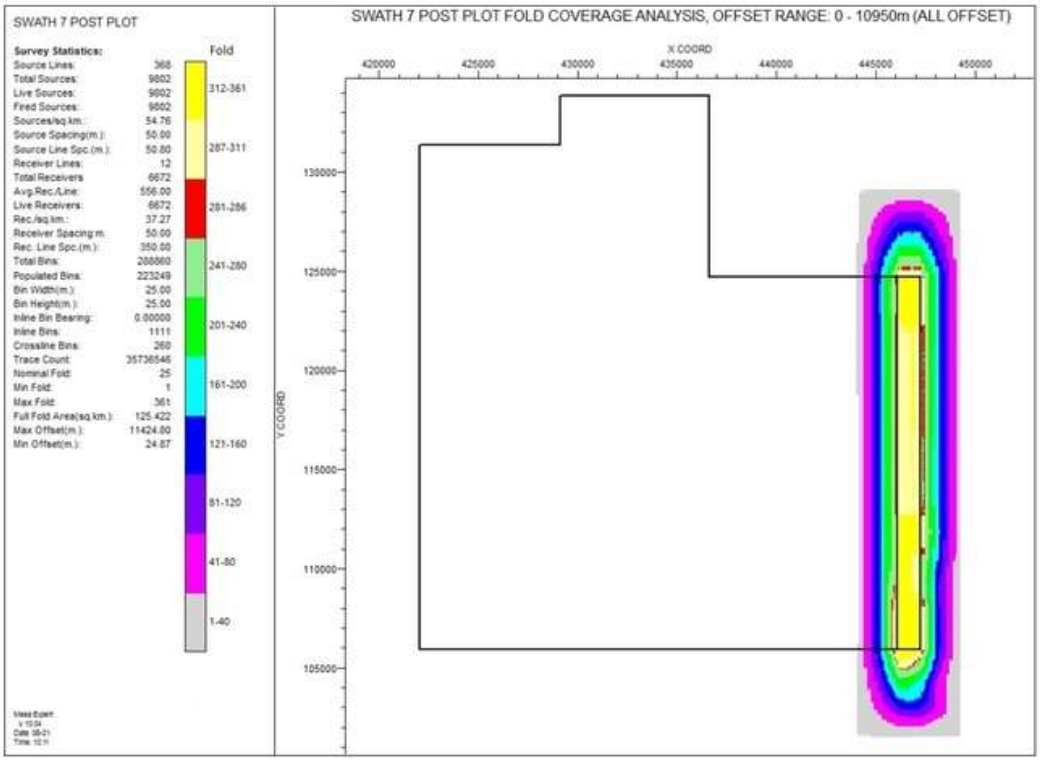

Figure 31**:** Swath 7 all offset fold coverage (0 - 10950m)

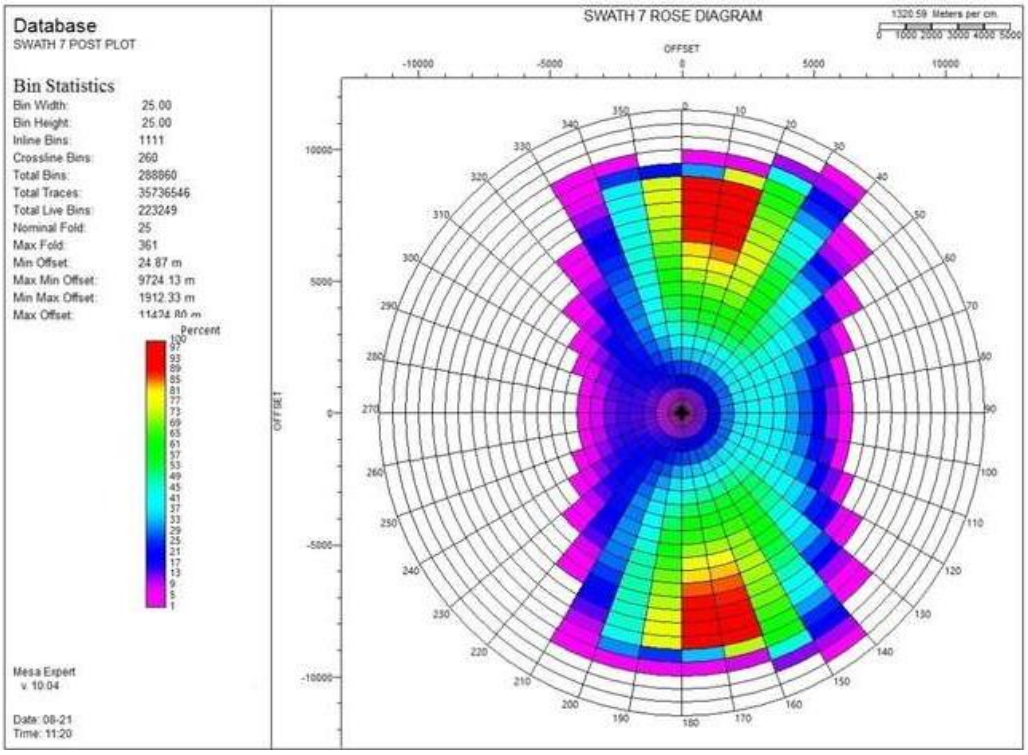

Figure 32: Swath 7 Rose diagram

Table 2 shows the horizontal extent (X-coordinate) of swaths and their folds and as well as areas with full fold coverage within a given swath.

Table 2: Extent of fold coverage for all swaths

Swath	X - coordinate (entire swath)		X - coordinate (area with full fold)	
	Beginning of fold	Ending of fold	Beginning of full fold	Ending of full fold
1	418500	425500	419000	423500
2	423000	429500	423500	428500
3	427000	433500	428500	432500
4	431000	438000	432500	436500
5	435500	442000	436500	441000
6	440000	446000	441000	445000
7	443500	449500	445000	448500

Fold coverage interpretation and implication

The minimum fold coverage required for every bin in this project is one hundred and eighty (180). Therefore, any fold coverage within the acquisition setting or study area that falls below the set fold standard for this project is not acceptable and should be beefed up to the minimum required fold to achieve the objective of the project convincingly, which include amongst others, the improvement of sub-surface structural imaging of the study area.

This fold coverage analysis for the project was carried out with respect to each swath in three (3) phases. These phases are the near offset fold coverage (0 – 3650m), the mid offset fold coverage (3650 – 7300m) and the far offset fold coverage (7300 – 10950m). Later, these fold coverage phases were merged to see if the fold coverage of each swath meets the minimum fold coverage requirement of 180, with respect to the number of shots planned per swath.

Figures 8, 13, 18, 23 and 28, which represent the near offset fold coverage for the selected swaths, it was observed that none of them met the minimum standard fold coverage set out for this project as the maximum fold values observed within the near offset range are 111, 151, 165, 131 and 122 respectively. This is likely as a result of shooting from one end of the swath as all the shot points being acquired may not fall within the swath receiver lines or are a bit separated from the swath receiver lines. Swath receiver lines are primarily centered within the swath and points to be acquired,

depending on the design of the project, most often extends beyond both ends of swath receivers as in this case.

Figures 9, 14, 19, 24 and 29 represent the mid offset fold coverage for the selected swaths. It was observed here that stipulated fold coverage standard for the project was slightly met as compared to the number of shots involved and the area of fold coverage. The small area that met the required fold standard for the project with respect to mid offset range shots for various swaths are bounded at 105000 – 132500 on the Y–Coordinate and 425000 – 425800 on the X-Coordinate for Figure 9; 106000 – 133000 on Y-Coordinate and 428500 – 431500 on X-Coordinate for Figure 14; 1035000 – 134000 on Y-Coordinate and 433000 – 436000 on X-Coordinate for Figure 19; 105000 – 127000 on Y-Coordinate and 437000 – 440000 on X-Coordinate for Figure 24; 105000 – 127000 on Y-Coordinate and 445000 – 447000 on X-Coordinate for Figure 29. The few bins observed to have accumulated the minimum required fold coverage within the mid offset range are likely as a result of most reflected shots being captured by the receivers as majority of the shots is not reflected away from the swath receivers due to their position at the middle of the swaths under consideration. This situation is quite different when compared to near and far offset ranges. It is worthy of note that the shots at both near and far offset ranges as the case may be, and their positions as well, can contribute to the fold coverage of other swaths as reflected shots maybe captured by the receivers of other swaths (Chong Zeng. et al. 2016). This is because reflections take place in diverse directions. In this case, we consider what is called swath overlap, as some shot points seen to be contributing to fold building in one swath, contributes to the fold coverage of another swath as well because of their positions. These types of shot points are commonly seen at the near and far offset ranges of any given swath (Sanchez-Ferrer et al. 1999).

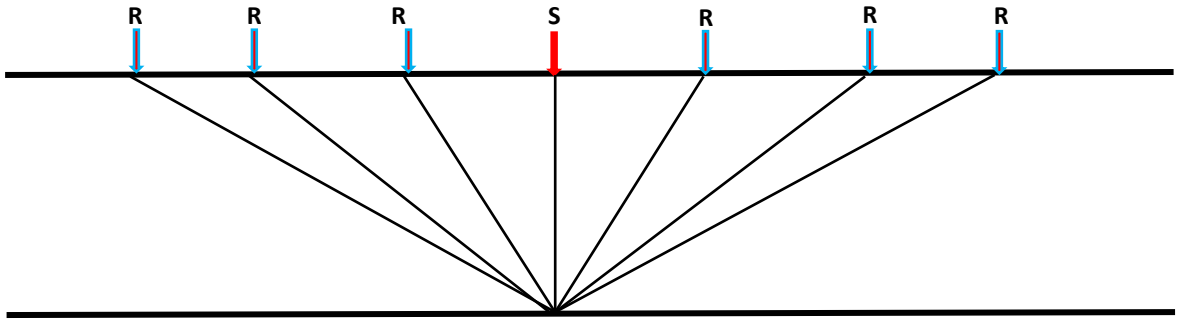

Figure 33: Shots reflected in diverse directions

With respect to far offset which is represented in Figs. 11, 15, 20, 25 and 30, it was clearly observed that the maximum fold coverage for the swaths except for Figure 20, are 122, 166, 127 and 112 respectively and they fall below the fold expectancy of the project. In Figure 20, we observed some bins having fold coverage of above 180, which is the set standard for the project. The maximum fold value observed in in Figure 20 is 191. The bins with fold value above 180 are situated between 105500 – 133500 on Y-coordinate and 433000 – 437000 on X-coordinate. Within the coordinate that is observed to have fold coverage of 180 and above, there is a possibility that all the planned shots within it were acquired. This implies that there is little or no presence of non-seismic objects within the zone which could interrupt acquisition.

It has been clearly observed that considering the near offset fold coverage, mid offset fold coverage and far offset fold coverage for all the swaths separately, the fold coverage expectancy of all the bins in individual swaths cannot be reached, hence the need to merge the near offset fold coverage, mid offset fold coverage and far offset fold coverage for each swath to get the bins within each of the swaths sampled the minimum number of times required. Figures 11, 16, 21, 26 and 31 show the full fold coverage for each swath under consideration. In this case, all offset ranges 0 – 3650m for near offset, 3650 – 7300m for mid offset and 7300 – 10950m for far offset are merged to have 0 – 10950m for full fold coverage of each swath. The maximum fold coverage observed for all offset ranges combined for individual swath are 358, 420, 446, 381 and 361 respectively. These maximum folds observed for each swath is twice or above twice the minimum fold value estimated for each bin to be sampled within the study area. It was also observed from Figs.11, 16, 21, 26 and 31 that a very large area, if not almost all area within each given swath, met the minimum fold requirement for each bin within the various swaths. These areas with full fold coverage for individual swaths under consideration are situated between 103000 – 133000 on Y-coordinate and 423500 – 428500 on X-coordinate for Figure 11; 102500 – 135000 on Y-coordinate and 428500 – 432500 on X-coordinate for Figure 16; 103500 – 13500 on Y-coordinate and 432500 – 436500 on X-coordinate for Figure 21; 102500 -128000 on Y-

coordinate and 436500 441000 on X-coordinate for Figure 26; 101500 – 129000 0n Y-coordinate and 445000 – 448500 on X-coordinate for Figure 31.

CONCLUSION

From Table 2, it was observed that where full fold coverage of one swath ends, the full fold of the swath next to it commences. This shows that for the entire study area, every bin within all the swaths were sampled appropriately with respect to the minimum fold each bin should have. Though within the swaths, there are few bins whose fold falls below the 180 minimum fold set value for each bin within the study area as seen in Figs.11, 16, 21, 26 and 31 respectively. This fold drop observed within these bins is as a result of non-seismic objects found within the acquisition area. Some of these affected shot points which were not acquired in order not to have a negative impact on the environment as well as non-seismic objects or bodies, are moved to safe positions within the swath and acquired to compensate for the fold drop. Where these shots cannot be moved to safe positions, they are completely killed and infill shots are planted to compensate for the fold drop.

It should be noted that certain natural, human and logistics limitations were encountered in this study. During this project, weather posed a great threat. This includes cloudy conditions and rainfall. The cloudy conditions resulted in statics within the atmosphere, which affected some acquired shots by destructive interference. Other natural conditions which made acquisition a bit difficult were the swampy terrain as it inhibited movement on the lines, wildlife like bees; reptiles etc as acquisition were mostly carried out in the forest and swamps. Human errors and most often the not readily available experience hands to guide the acquisition process somehow delayed the process. The study area is about 60% upland and 40% marine. Sometimes, it was difficult to navigate to the desired area of interest within the study sites.

ACKNOWLEDGEMENTS

I want to Acknowledge Bureau of Geophysical Prospecting (BGP) Nigeria Limited—Crew 8619—for making their facility available for this research.

Data availability: The data that support the findings of this study are available on request from the corresponding author.

Conflict of interest: The authors declare that they have no conflict of interest to declare.

Ethical approval: The paper reflects the authors' research and analysis in a truthful and complete manner.

REFERENCES

Claerbout, J. F. (1976). Fundamentals of geophysical data processing: McGraw-Hill Book Co.

Cordsen, A., Lawton, D. C. (1996). Designing 3-component 3D seismic surveys. 66th Annual International Meeting, SEG, Expanded Abstracts 81–83

Cordsen, A., Galbraith, M., Peirce, J. (2000). Planning land 3-D seismic surveys. Society of Exploration Geophysicists, 204. http://dx.doi.org/10.1190/1.9781560801801

Gadallah, M. R., Fisher, R. (2009). Exploration geophysics. Springer Berlin

Galbraith, M., (2001). 3D Seismic Surveys – Past, Present and Future. Canadian Society of Exploration Geophysicist. 26(6)

Geoscience Training Center, (2002). Land acquisition 2D and 3D geometry

Goodway, W.N., Ragan, B., (1995). Focused 3D: consequences of mid-point scatter and spatial sampling in acquisition design, processing and interpretation. Ann Mtg Can Soc Expl Geoph Expanded Abstracts, 177-178

Krey, ThC (1987). Attenuation and random noise by 2D and 3D CDP stacking and Kirchhoff migration. Geophysical Prospecting, 35(2):135-147

O'Connell, J.K., Kohli, M. and Amos, S., 1993, Bullwinkle: a unique 3-D experiment: Geophysics, 58, No. 1, 167-176.

Sanchez-Ferrer, F., James, S.D., Lak, B., Evans, A.M., (1999). Techniques use in the exploration of turbidite reservoirs in frontier settings – Helland Hansen licence, Vøring Basin, offshore Mid-Norway. In: Fleet AJ, Boldy SAR (eds) Petroleum geology of North West Europe. Proceedings of the 5th Conference, Geological Society of London 281-292

Yilmaz, O. (2001). Seismic data analysis: processing, inversion, and interpretation of seismic data. Society of Exploration Geophysicists Tulsa, OK 1028. https://doi.org/10.1190/1.9781560801580

Zeng, C., Dong, S., Wang, B., (2016). Adaptive least-squares RTM with applications to subsalt imaging. The Leading Edge 35(3):253-257. DOI: 10.1190/TLE35030253.1